

Direct observation of the ground state of a 1/3 quantum magnetization plateau in $\text{SrMn}_3\text{P}_4\text{O}_{14}$ using neutron diffraction measurements

Masashi Hase^{1*}, Vladimir Yu. Pomjakushin², Andreas Dönni¹, Tao Yang³, Rihong Cong³, and Jianhua Lin³

¹*National Institute for Materials Science (NIMS), Tsukuba, Ibaraki 305-0047, Japan*

²*Laboratory for Neutron Scattering, Paul Scherrer Institut (PSI), CH-5232 Villigen PSI, Switzerland*

³*College of Chemistry and Molecular Engineering, Peking University, Beijing 100871, People's Republic of China*

We can directly investigate the ground state in magnetization-plateau fields (plateau ground state) using neutron diffraction measurements. We performed neutron diffraction measurements on the spin-5/2 trimer substance $\text{SrMn}_3\text{P}_4\text{O}_{14}$ in magnetization-plateau fields. The integrated intensities of magnetic reflections calculated using an expectation value of each spin in a plateau ground state of an isolated-trimer model agree well with those obtained experimentally in the magnetization-plateau fields. We succeeded in direct observation of a plateau ground state in $\text{SrMn}_3\text{P}_4\text{O}_{14}$.

1. Introduction

During typical quantum-mechanics calculations, we first calculate eigenstates and eigenenergies of a model Hamiltonian and then calculate physical quantities such as magnetization and specific heat. We compare the experimentally obtained physical quantities of a substance and those calculated in a hypothesized model Hamiltonian. Then we judge whether the hypothesized model is applicable to the substance. We do not usually investigate the eigenstates themselves directly in experiments.

We can directly investigate a ground state in magnetic fields where a quantum magnetization plateau appears (plateau ground state) using neutron diffraction measurements as explained below.¹ Before providing an explanation, we describe a quantum

*HASE.Masashi@nims.go.jp

magnetization plateau.^{2,3} The magnetization of a plateau ground state takes its maximum value because of the magnetic fields. Excited states cannot contribute to magnetization because of energy gaps separating the plateau ground state and excited states. Therefore, magnetization cannot increase and the quantum magnetization plateau appears.

The existence of an energy gap is important for the occurrence of a quantum magnetization plateau. It can be confirmed using other methods. A zero-magnetization plateau appears in spin systems possessing spin-singlet ground state(s) and a spin gap separating the ground and first-excited states. Examples are Haldane substances,^{4,5} the spin-Peierls cuprate CuGeO_3 ,⁶ and the orthogonal-dimer compound $\text{SrCu}_2(\text{BO}_3)_2$.⁷ It is possible to prove the existence of a spin gap explicitly by the exponential decay of magnetic susceptibility on cooling.⁷⁻¹⁰ Inelastic neutron scattering (INS) techniques are useful not only for a spin gap generating a zero-magnetization plateau, but also for an energy gap generating a finite-magnetization plateau. The existence of an energy gap generating a finite-magnetization plateau was confirmed in NH_4CuCl_3 ,¹¹ $\text{Cu}_3(\text{P}_2\text{O}_6\text{OD})_2$,¹² and $\text{SrMn}_3\text{P}_4\text{O}_{14}$.¹³

In a plateau ground state, a magnetic moment on each site must be fully polarized parallel and anti-parallel to external magnetic fields when $\langle S_{jz} \rangle$ value on the site is positive and negative, respectively.¹⁴ Here, $\langle S_{jz} \rangle$ is an expectation value of spin on an j -th magnetic-ion site in the plateau ground state. The full polarizations generate the magnetization plateau. We can determine a value of $g\mu_B\langle S_{jz} \rangle$ (a value of a magnetic moment) in magnetization-plateau fields from magnetic reflections obtained in neutron diffraction measurements. Therefore, we can compare theoretical and experimental values of $\langle S_{jz} \rangle$, meaning that direct investigation of a plateau ground state can be done through neutron diffraction measurements.

Magnetization plateaus, however, are usually apparent in high magnetic fields or at extremely low temperatures. Therefore, neutron diffraction measurements of plateau ground states are usually difficult. They have not been reported in the literature to date.

A 1/3 quantum magnetization plateau is apparent between 2 and 10 T at 1.3 K in insulating $\text{SrMn}_3\text{P}_4\text{O}_{14}$.^{15,16} Therefore, it is possible to perform neutron diffraction measurements of the substance in magnetization-plateau fields. Here, we describe the crystal structure and magnetism of $\text{SrMn}_3\text{P}_4\text{O}_{14}$. The space group is monoclinic $P2_1/c$ (No. 14).¹⁵ The lattice constants at 4.0 K are $a = 7.661(1) \text{ \AA}$, $b = 7.784(1) \text{ \AA}$, $c = 9.638(1)$

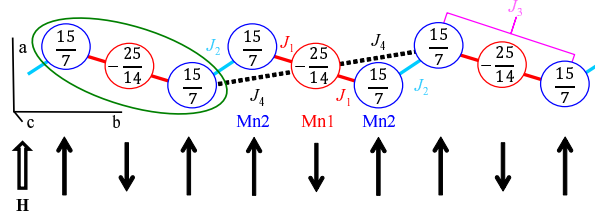


Fig. 1. (Color online) The spin system in $\text{SrMn}_3\text{P}_4\text{O}_{14}$.¹⁶ Mn^{2+} ions ($3d^5$) have localized spin $5/2$. Two kinds of Mn sites (Mn1 and Mn2) exist. The major AF J_1 interaction forms spin trimers as shown by the ellipse. Considering J_i ($i = 1 \sim 4$) interactions, we can explain a coplanar spiral magnetic structure below $T_N = 2.2(1)$ K in the zero magnetic field.¹⁷ The values on Mn sites show $\langle S_{jz} \rangle$ in the plateau ground state in the isolated trimer. Arrows depict schematically magnetic moments ($g\mu_B \langle S_{jz} \rangle$) in the plateau ground state obtained in the present study.

\AA , and $\beta = 111.70(2)^\circ$.¹⁷ Two Mn^{2+} sites (Mn1 and Mn2) exist as presented in Fig. 1. The electron configuration in Mn^{2+} ions is $3d^5$. Anisotropy in exchange interactions is caused by the spin-orbit interaction and a low symmetry of crystal fields. The spin value on Mn^{2+} ions in this substance is $5/2$.¹⁶ Therefore, the orbital moment is 0. The spin-orbit interaction and single ion anisotropy do not exist. The g -value is isotropic and about 2. We evaluated experimentally that the powder-average g -value was 1.98 from the saturated value of magnetization ($4.95\mu_B$ per Mn). The Mn atoms are coordinated octahedrally by six oxygen atoms. The symmetry of crystal fields affecting the Mn^{2+} ions is nearly cubic. Accordingly, the anisotropy in exchange interactions of Mn spins in this substance is expected to be small. We can consider that spin- $5/2$ on Mn^{2+} ions is a Heisenberg spin.

We can explain magnetizations¹⁶ and magnetic excitations observed in INS experiments¹³ using an isolated antiferromagnetic (AF) Heisenberg spin- $5/2$ trimer. The trimer indicated by the ellipse in Fig. 1 is formed by the AF J_1 interaction. The value of J_1 was estimated as $3.4 \sim 4.0$ K.^{13,16} A coplanar spiral magnetic structure appears below $T_N = 2.2(1)$ K in the zero magnetic field.¹⁷ Therefore, other exchange interactions are not negligible. The spiral magnetic structure results from frustration between nearest-neighbor and next-nearest-neighbor exchange interactions in the trimerized chain formed by J_i ($i = 1 \sim 4$) interactions.

In the isolated-trimer model, states with $\langle (\mathbf{S}^T)^2 \rangle = \frac{5}{2}(\frac{5}{2}+1)$ and $E/J_1 = -15$ are six-folded ground states in 0 T where \mathbf{S}^T and E represent the sum of three spin operators in a trimer and eigenenergy per three spins, respectively. In magnetic fields up to 10 T,

one ground state with $\langle S_z^T \rangle = 5/2$ is the unique ground state. In the ground state, each $\langle S_{jz} \rangle$ value was calculated as $\langle S_{1z} \rangle = -25/14$ and $\langle S_{2z} \rangle = 15/7$ on Mn1 and Mn2 sites, respectively. As shown in Fig. 1, the spin on Mn1 (Mn2) site is anti-parallel (parallel) to magnetic fields in magnetization-plateau fields. Therefore, the 1/3 magnetization plateau appears ($\langle S_z^T \rangle = \langle S_{1z} \rangle + 2\langle S_{2z} \rangle = 5/2$).

We performed neutron diffraction measurements of $\text{SrMn}_3\text{P}_4\text{O}_{14}$ in magnetic fields. In analyses, we assumed that the plateau ground state in $\text{SrMn}_3\text{P}_4\text{O}_{14}$ was close to that in the isolated AF spin-5/2 trimer. Experimental integrated intensities of magnetic reflections are consistent with integrated intensities of magnetic reflections calculated using $\langle S_{jz} \rangle$ values expected in the isolated trimer ($\langle S_{1z} \rangle = -25/14$ and $\langle S_{2z} \rangle = 15/7$).

2. Methods of Experiments

Single crystals of $\text{SrMn}_3\text{P}_4\text{O}_{14}$ were synthesized under hydrothermal conditions at 473 K. Details of the synthesis have been reported elsewhere.¹⁵ Each crystal was small. For that reason, we pulverized crystals. We entered powders in paraffin molten by heating and embedded the powders in solid paraffin. We measured magnetizations of the powders embedded in solid paraffin up to $H = 5$ T and down to 1.8 K using a superconducting quantum interference device (SQUID) magnetometer (MPMS-5S; Quantum Design).

We conducted neutron diffraction experiments at the Swiss spallation neutron source (SINQ) in Paul Scherrer Institut (PSI). We used the high-resolution powder diffractometer for thermal neutrons HRPT.¹⁸ The wave length λ was 2.45 Å. Magnetic fields of 0 - 6 T were applied almost perpendicular to the scattering plane using a superconducting magnet. The deviation from 90° of the angle between the scattering vector \mathbf{Q} and magnetic field \mathbf{H} is less than 6° ($\cos 6^\circ = 0.995$). We used pressed pellets of $\text{SrMn}_3\text{P}_4\text{O}_{14}$ to minimize the problem of powder realignment in strong magnetic fields. We performed Rietveld refinements of the crystal structure using the `FULLPROF Suite` program package,¹⁹ using its internal tables for scattering lengths.

3. Results and discussion

The circles in Fig. 2(a) show a neutron diffraction pattern of $\text{SrMn}_3\text{P}_4\text{O}_{14}$ pellets at 20 K in 0 T (paramagnetic state). We performed Rietveld refinements of the crystal structure. We assume that directions of domains are randomly distributed both in the present (pellet) and previous (powder) samples.¹⁷ The line on the experimental pattern

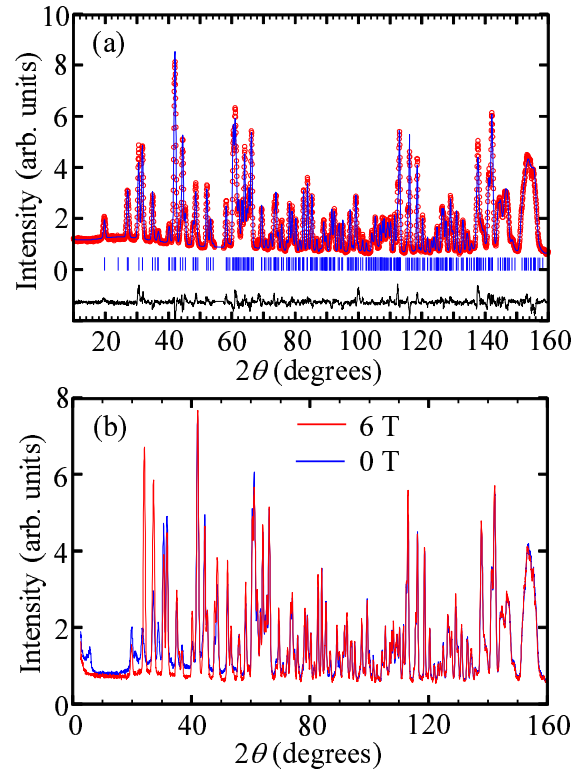


Fig. 2. (Color online) Neutron diffraction patterns of $\text{SrMn}_3\text{P}_4\text{O}_{14}$ pellets measured using the HRPT diffractometer ($\lambda = 2.45 \text{ \AA}$). (a) Circles show a diffraction pattern measured at 20 K in 0 T. Lines on the measured pattern and at the bottom portray a Rietveld refined pattern and the difference between the measured and the Rietveld refined patterns, respectively. Hash marks represent the positions of nuclear reflections. (b) Neutron diffraction patterns at 1.6 K in 0 and 6 T.

indicates the result of Rietveld refinements. It can explain the experimental pattern. Structural parameters obtained in the present refinements are consistent with those obtained in the previous refinements. Therefore, no alignment of powders occurs in producing the pellets. Figure 2(b) shows diffraction patterns of pellets at 1.6 K in 0 and 6 T. The two diffraction patterns are mutually close at high angles, indicating that no alignment of powders in the pellets occurs by application of magnetic fields.

Figure 3 depicts fragments of neutron diffraction patterns of $\text{SrMn}_3\text{P}_4\text{O}_{14}$ pellets at 1.6 K in several magnetic fields. Open blue circles under the patterns denote positions of major magnetic reflections generated by the spiral magnetic structure.¹⁷ The intensities decrease concomitantly with increasing magnetic field H and disappear in $H \geq 0.3 \text{ T}$. The positions of the magnetic reflections are independent of H . The spiral magnetic order results from the AF J_1 interaction ($3.4 \sim 4.0 \text{ K}$) and other weaker interactions in

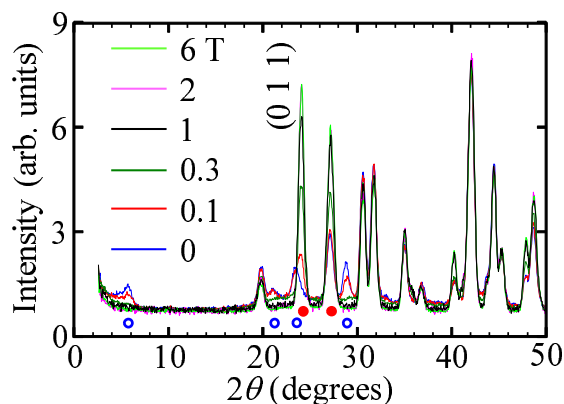


Fig. 3. (Color online) Neutron diffraction patterns of $\text{SrMn}_3\text{P}_4\text{O}_{14}$ pellets at 1.6 K in several magnetic fields measured using the HRPT diffractometer ($\lambda = 2.45 \text{ \AA}$). Open blue circles represent positions of major magnetic reflections generated by the spiral magnetic structure. Closed red circles represent positions of major magnetic reflections with integer indices appearing in $H \geq 0.05 \text{ T}$.

the quasi-one-dimensional system in Fig. 1. The order is easily destroyed by the weak magnetic fields.

Closed red circles under the patterns in Fig. 3 indicate positions of major new magnetic reflections with integer indices appearing in $H \geq 0.05 \text{ T}$. Figure 4 shows the integrated intensity of the (0 1 1) reflection at $2\theta = 24.1^\circ$. Figure 4(a) shows that the intensity is strong in high magnetic fields and at low temperatures. Figure 4(b) shows that the intensity at 1.6 K (open red circle) increases concomitantly with increasing H and that it is almost independent of H above 2 T. The H dependence is similar to that of square of magnetization measured at 1.8 K (closed blue circle). Therefore, the new reflections are correlated with the $1/3$ quantum magnetization plateau. Figure 4(c) shows that the intensity in 6 T (open red circle) decreases with increasing temperature T and that it is negligible at 20 K. The T dependence of a normalized order parameter is usually expressed as $(1 - T/T_c)^\beta$ ($0 < \beta < 1$) just below a transition temperature T_c . The T dependence of the intensity in 6 T differs from that of an order parameter, indicating that no phase transition occurs. The state in $H \geq 0.3 \text{ T}$ is a polarized paramagnetic state without spontaneous magnetic order. The magnetic reflections are generated by magnetic moments aligned parallel or anti-parallel to the applied magnetic fields. The T dependence of the (0 1 1) intensity is inconsistent with that of square of magnetization measured in 5 T (closed blue circle). Magnetic reflections are generated by static magnetic moments, whereas magnetization is determined both by static magnetic moments

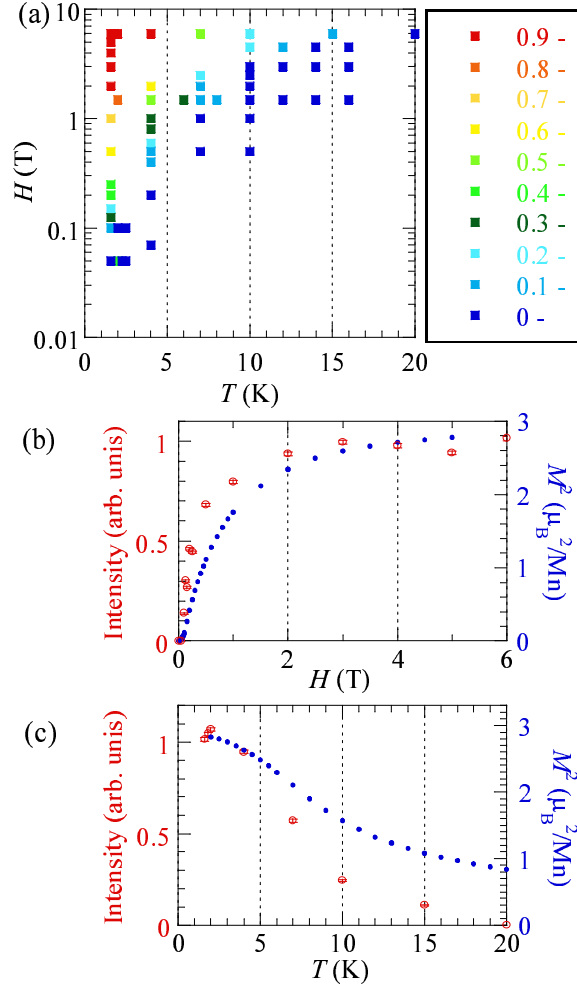


Fig. 4. (Color online) (a) The integrated intensity map of the (0 1 1) reflection in the $T - H$ plane. The right panel shows intensity in arbitrary units. (b) The magnetic-field dependence of the integrated intensity of the (0 1 1) reflection at 1.6 K (open red circle). Closed blue circles show the square of magnetization measured at 1.8 K. (c) Temperature dependence of the integrated intensity of the (0 1 1) reflection in 6 T (open red circle). Closed blue circles represent square of magnetization measured in 5 T.

and paramagnetic components. Therefore, the inconsistency appears. In Fig. 3, diffuse scattering is apparent at $2\theta = 20 \sim 34^\circ$ in low magnetic fields, but it disappears in $H \geq 1$ T. The diffuse scattering stems from short-range magnetic correlations in the low-dimensional spin system. With increasing magnetic field, the short-range magnetic correlations are weakened and are replaced by long-range magnetic correlations (the polarized paramagnetic state).

We obtained integrated intensities of nuclear reflections in the diffraction pattern at 1.6 K in 0 T. We calculated integrated intensities of nuclear reflections $[I_N(\mathbf{Q})]$ using

the following.

$$I_N(\mathbf{Q}) = A|F_N(\mathbf{Q})|^2 n_{\mathbf{Q}} \frac{1}{\sin 2\theta \sin \theta}. \quad (1)$$

Therein,

$$F_N(\mathbf{Q}) = \sum_j b_j \exp(i\mathbf{Q} \cdot \mathbf{r}_j) \exp(-B_j \frac{\sin^2 \theta}{\lambda^2}). \quad (2)$$

A is a scaling coefficient. $n_{\mathbf{Q}}$ is the number of reflections having the same intensity and $|\mathbf{Q}|$. b_j is a scattering length of the j -th site atom. The values of b_j are 7.02×10^{-13} , -3.75×10^{-13} , 5.13×10^{-13} , and 5.81×10^{-13} cm for Sr, Mn, P, and O, respectively.²⁰ \mathbf{r}_j is the position of the j -th site atom. B_j is an atomic displacement parameter. We used atomic positions and values of B_j determined in Rietveld refinements for a neutron diffraction pattern at 4.0 K in 0 T.¹⁷ Figure 5(a) portrays integrated intensities of nuclear reflections in the diffraction pattern at 1.6 K in 0 T versus corresponding calculated integrated intensities of nuclear reflections at $2\theta < 55^\circ$. We obtained $A = 2.25 \times 10^{24}$ cm⁻².

We obtained integrated intensities of reflections in the diffraction pattern at 1.6 K in 6 T. The intensities include nuclear and magnetic contributions. We defined that the difference of intensities between 6 T and 0 T at each reflection was an integrated intensity of a magnetic reflection in magnetization-plateau fields. We calculated the integrated intensities of magnetic reflections $[I_M(\mathbf{Q})]$ in a neutron powder diffraction pattern using the following:

$$I_M(\mathbf{Q}) = A|F_M(\mathbf{Q})|^2 n_{\mathbf{Q}} \frac{1}{\sin 2\theta \sin \theta}, \quad (3)$$

where

$$F_M(\mathbf{Q}) = -\frac{g}{2} \frac{\gamma e^2}{m_e c^2} \sum_j f(Q)_j \langle S_{jz} \rangle \exp(i\mathbf{Q} \cdot \mathbf{r}_j) \exp(-B_j \frac{\sin^2 \theta}{\lambda^2}). \quad (4)$$

The g value is 1.98. The value of $\frac{\gamma e^2}{m_e c^2}$ is 5.39×10^{-13} cm. $f(Q)_j$ is a magnetic form factor of a j -th site ion.²¹ The direction of magnetic fields is always almost perpendicular to \mathbf{Q} in the experimental setup. As described, in a plateau ground state, a magnetic moment on each site is fully polarized parallel and anti-parallel to external magnetic fields. Therefore, magnetic moments are always almost perpendicular to \mathbf{Q} . In Eq. (4), we can input the scalar $\langle S_{jz} \rangle$ instead of the vector $\mathbf{S}_{j\perp\mathbf{Q}}$ (components of \mathbf{S} perpendicular to \mathbf{Q}).

We assume that the plateau ground state in SrMn₃P₄O₁₄ is close to that in the

isolated AF spin-5/2 trimer as shown by the ellipse in Fig. 1. As described previously, in the plateau ground state in the isolated trimer, $\langle S_{1z} \rangle = -25/14$ on Mn1 site and $\langle S_{2z} \rangle = 15/7$ on Mn2 site, satisfying $\langle S_z^T \rangle = \langle S_{1z} \rangle + 2\langle S_{2z} \rangle = 5/2$. In a classical perspective, where magnitude of spin is constant, $\langle S_{1z} \rangle = -5/2$ and $\langle S_{2z} \rangle = 5/2$, also satisfying $\langle S_z^T \rangle = 5/2$. We can calculate integrated intensities of magnetic reflections without any refined parameters except for assumptions of $\langle S_{jz} \rangle$ values. Figure 5(b) presents calculated results versus experimental integrated intensities of magnetic reflections at $2\theta < 55^\circ$. The calculated results of the isolated trimer model agree well with the experimental results, whereas the calculated results of the classical model are larger than the experimental results. The value of $\langle S_z^T \rangle$ is constrained to be 5/2 because of the 1/3 quantum magnetization plateau. In the constraint, the calculated intensity of each magnetic diffraction decreases monotonically with decreasing $\langle S_{2z} \rangle$ value. The set of $\langle S_{1z} \rangle = -25/14$ and $\langle S_{2z} \rangle = 15/7$ is a unique solution that can explain the experimental results within experimental errors. Agreement between experimental and calculated results indicate that the plateau ground state in $\text{SrMn}_3\text{P}_4\text{O}_{14}$ is close to that in the isolated AF spin-5/2 trimer and that the ground state is almost unchanged by the other exchange interactions, except for the J_1 interaction.

We succeeded in direct observation of the plateau ground state in $\text{SrMn}_3\text{P}_4\text{O}_{14}$. Direct observation of the ground state was also conducted in $\text{Ca}_3\text{CuNi}_2(\text{PO}_4)_4$ in 0 T.^{22–24} The spin system is weakly coupled Ni-Cu-Ni trimers. In an isolated Ni-Cu-Ni trimer with single ion anisotropy $d(S_{\text{Ni}z})^2$ ($d < 0$), the ground states in the zero field are a doublet with $\langle S_z^T \rangle = \pm 3/2$. In the realistic model including effects of molecular fields from neighboring trimers, the unique expectation values of spin were calculated as $\langle S_{\text{Ni}z} \rangle = 0.9$ and $\langle S_{\text{Cu}z} \rangle = -0.3$. $\text{Ca}_3\text{CuNi}_2(\text{PO}_4)_2$ shows an AF order with an unusual multi- k magnetic structure below $T_N = 20$ K. The calculated expectation values of spin are in 10 % accuracy in agreement with experimental values of ordered spins.

In $\text{SrMn}_3\text{P}_4\text{O}_{14}$, the magnitudes of the ordered moments are 3.44 and 3.56 μ_B on Mn1 and Mn2 sites, respectively, at 1.5 K in 0 T.¹⁷ The ordered moments on Mn1 and Mn2 sites are almost mutually anti-parallel. The magnitude of the Mn1 moment is close to $g\mu_B|\langle S_{1z} \rangle| = 3.54\mu_B$, whereas the magnitude of the Mn2 moment is smaller than $g\mu_B|\langle S_{2z} \rangle| = 4.24\mu_B$. The sublattice magnetizations are not fully saturated at 1.5 K.¹⁷ The ground states in the isolated Mn2-Mn1-Mn2 trimer is six-folded in 0 T. Therefore, the ground states with $\langle S_z^T \rangle = \pm 3/2$ or $\langle S_z^T \rangle = \pm 1/2$ might affect the experimental values of the magnetic moments.

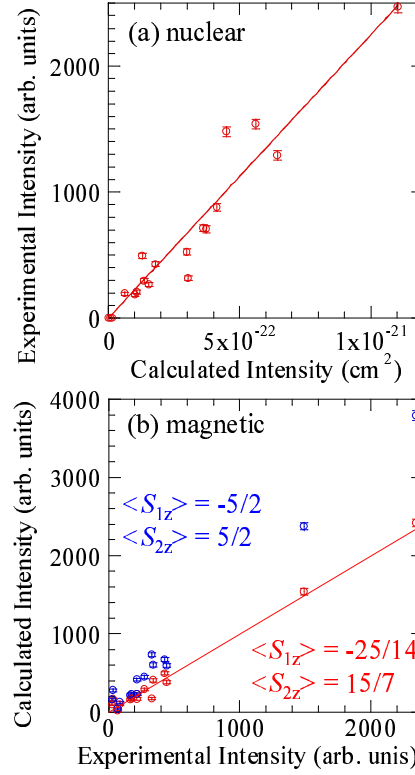


Fig. 5. (Color online) (a) Integrated intensities of nuclear reflections in the diffraction pattern at 1.6 K in 0 T versus calculated integrated intensities of nuclear reflections at $2\theta < 55^\circ$. (b) Integrated intensities of magnetic reflections calculated for $\langle S_{1z} \rangle = -25/14$ and $\langle S_{2z} \rangle = 15/7$ (red) and $\langle S_{1z} \rangle = -5/2$ and $\langle S_{2z} \rangle = 5/2$ (blue) versus experimental integrated intensities of magnetic reflections at $2\theta < 55^\circ$.

4. Conclusion

We performed neutron diffraction measurements on $\text{SrMn}_3\text{P}_4\text{O}_{14}$ pellets in magnetic fields to investigate the ground state in magnetization-plateau fields directly. The spin system is weakly coupled spin-5/2 trimers. Magnetic reflections indicating the occurrence of the coplanar spiral magnetic structure disappear in weak magnetic fields of $H \geq 0.3$ T. The result is consistent with the generation of the magnetic structure by weak exchange interactions (4.0 K at most) in the quasi-one-dimensional spin system. New magnetic reflections with integer indices appear in $H \geq 0.05$ T. They are correlated with the 1/3 quantum magnetization plateau. The temperature dependence of the integrated intensity of the new magnetic reflections differs from that of an order parameter. Therefore, the state in $H \geq 0.3$ T is a polarized paramagnetic state without spontaneous magnetic order. The integrated intensities of the magnetic reflections calculated using

the expectation values of spins in the plateau ground state in the isolated-trimer model agree well with those obtained experimentally in the magnetization-plateau fields. We succeeded in direct observation of the plateau ground state in $\text{SrMn}_3\text{P}_4\text{O}_{14}$.

Acknowledgment

This work was supported by KAKENHI (No. 23540396) and by grants from NIMS. The neutron powder diffraction experiments were conducted at SINQ, PSI Villigen, Switzerland (Proposal Nos. 20111258 and 20130552). We are grateful to K. Kaneko for invaluable discussion and to S. Matsumoto for producing pellets.

References

- 1) Strictly speaking, we cannot see a ground state itself at finite temperatures because of thermal mixing of excited states. However, the influence of excited states is negligible in magnetization-plateau fields because of an energy gap.
- 2) K. Hida, J. Phys Soc. Jpn. **63**, 2359 (1994).
- 3) M. Oshikawa, M. Yamanaka, and I. Affleck, Phys. Rev. Lett. **78**, 1984 (1997).
- 4) K. Katsumata, H. Hori, T. Takeuchi, M. Date, A. Yamagishi, and J. P. Renard, Phys. Rev. Lett. **63**, 86 (1989).
- 5) Y. Ajiro, T. Goto, H. Kikuchi, T. Sakakibara, and T. Inami, Phys. Rev. Lett. **63**, 1424 (1989).
- 6) M. Hase, I. Terasaki, K. Uchinokura, M. Tokunaga, N. Miura, and H. Obara, Phys. Rev. B **48**, 9616 (1993).
- 7) H. Kageyama, K. Yoshimura, R. Stern, N. V. Mushnikov, K. Onizuka, M. Kato, K. Kosuge, C. P. Slichter, T. Goto, and Y. Ueda, Phys. Rev. Lett. **82**, 3168 (1999).
- 8) J. P. Renard, M. Verdaguer, L. P. Regnault, W. A. C. Erkelens, J. Rossatmignod, and W. G. Stirling, Europhys. Lett. **3**, 945 (1987).
- 9) M. Hase, I. Terasaki, and K. Uchinokura, Phys. Rev. Lett. **70**, 3651 (1993).
- 10) M. Hase, I. Terasaki, Y. Sasago, K. Uchinokura, and H. Obara, Phys. Rev. Lett. **71**, 4059 (1993).
- 11) Ch. Rüegg, M. Oettli, J. Schefer, O. Zaharko, A. Furrer, H. Tanaka, K. W. Kramer, H. U. Gudel, P. Vorderwisch, K. Habicht, T. Polinski, and M. Meissner, Phys. Rev. Lett. **93**, 037207 (2004).
- 12) M. Hase, M. Matsuda, K. Kakurai, K. Ozawa, H. Kitazawa, N. Tsujii, A. Dönni, M. Kohno, and X. Hu, Phys. Rev. B **76**, 064431 (2007).
- 13) M. Hase, M. Matsuda, K. Kaneko, N. Metoki, K. Kakurai, T. Yang, R. Cong, J. Lin, K. Ozawa, and H. Kitazawa, Phys. Rev. B **84**, 214402 (2011).
- 14) As described herein, it is defined that the sign of a magnetic moment is positive (negative) when the sign of a spin value is positive (negative).
- 15) T. Yang, Y. Zhang, S. Yang, G. Li, M. Xiong, F. Liao, and J. Lin, Inorg. Chem. **47**, 2562 (2008).

- 16) M. Hase, T. Yang, R. Cong, J. Lin, A. Matsuo, K. Kindo, K. Ozawa, and H. Kitazawa, Phys. Rev. B **80**, 054402 (2009).
- 17) M. Hase, V. Yu. Pomjakushin, L. Keller, A. Dönni, O. Sakai, T. Yang, R. Cong, J. Lin, K. Ozawa, and H. Kitazawa, Phys. Rev. B **84**, 184435 (2011).
- 18) P. Fischer, G. Frey, M. Koch, M. Koennecke, V. Pomjakushin, J. Schefer, R. Thut, N. Schlumpf, R. Buerge, U. Greuter, S. Bondt, and E. Berruyer, Physica B, **276-278**, 146 (2000); <http://sinq.web.psi.ch/hrpt>
- 19) J. Rodriguez-Carvajal, Physica B (Amsterdam) **192**, 55 (1993); <http://www.ill.eu/sites/fullprof/>.
- 20) A. Rauch and W. Waschkowski, chapter 1.1 (Neutron scattering lengths), Neutron Data Booklet (Edited by A.-J. Dianoux and G. Lander), Neutrons for Science, Institut Laue-Langevin.
- 21) S. W. Lovesey, Theory of Neutron Scattering from Condensed Matter Vol.2, Oxford University Press (1984).
- 22) V. Yu Pomjakushin, A. Furrer, D. V. Sheptyakov, E. V. Pomjakushina, and K. Conder, Phys. Rev. B **76**, 174433 (2007).
- 23) V. Pomjakushin, arXiv:1404.1683.
- 24) A. Podlesnyak, V. Pomjakushin, E. Pomjakushina, K. Conder, and A. Furrer, Phys. Rev. B **76**, 064420 (2007).